MOLECULAR PHYSICS REPORTS 28 (2000) 37-43

EPR STUDIES OF THE HIGH TEMPERATURE PHASE OF $MgSiF_6 \cdot 6H_2O:Mn^{2+}$

W. ZAPART[1], M. B. ZAPART[1], A. M. ZIATDINOV[2]

[1] *Institute of Physics, Technical University, Al. Armii Krajowej 19, 42-200 Częstochowa, Poland*
[2] *Institute of Chemistry, Far Eastern Branch of the Russian Academy of Sciences, Vladivostok, Russia*

Abstract: The EPR lineshape analysis in $MgSiF_6 \cdot 6H_2O$ in its high temperature phase is presented using two models – incommensurably modulated structure and antiphase domain structure. The comparison between observed EPR spectra and theoretically predicted EPR lineshapes by both models is given. Since neither rentgenographic nor neutronographic studies have revealed the presence of superstructure reflections in incommensurate positions the latter model with a discrete variable has been taken into consideration. The presented approach describes the experimental EPR spectra quite well and is consistent with the structural model of $MgSiF_6 \cdot 6H_2O$ above T_c proposed in the literature.

Modulated (commensurate and incommensurate) structures form an important class of structures observed among all categories of materials. The modulations can involve a continuous variable (for example the atomic position in the case of displacive modulations) or a discrete variable which takes a finite number of values (long-period antiphase boundary structures). Two kinds of models have been proposed for antiphase boundary (APB) structures: the first assuming sharp domain walls strictly contained in crystal planes [1] and the second taking into account wavy antiphase boundaries [2].

These structures can be studied within the general Landau-Ginzburg theory of phase transitions [3]. In this framework they consist of commensurate regions separated by discommensurations or solitons. These solitons can correspond to the wide antiphase boundaries at high temperatures. At lower temperatures the solitons become narrower and pinned to the lattice so that commensurate structures can appear through a lock-in transition. At intermediate temperatures complex structures can appear with the possible occurrence of devil's staircase [3]. The structures can all be described using more or less smoothed square wave functions, the smoothing being a function of temperature.

In crystals belonging to a family of the type $ABF_6 \cdot 6H_2O$ the existence of regular antiphase domain structure has been reported in their high temperatures phases [4]. The EPR spectra of admixture ions observed in this temperature range resemble those evidenced in incommensurate systems [5].

1. THE STRUCTURAL MODEL OF HIGH TEMPERATURE PHASE OF $MgSiF_6 \cdot 6H_2O$ CRYSTAL

Magnesium fluosilicate hexahydrate $MgSiF_6 \cdot 6H_2O$ (MFSH) belongs to a crystal family of the type $ABF_6 \cdot 6H_2O$ where A is a divalent iron group metal ion (Fe, Co, Ni, Zn, Mn) and B is a quadrivalent element like Si, Sn, Ti, Ge. The $ABF_6 \cdot 6H_2O$ system is of interest since most of its members undergo structural phase transitions below room temperature which have been investigated by different macroscopic and microscopic methods [5-13]. The rhombohedrally

distorted CsCl-type structure of these compounds is composed of columns made up with alternating $[A(H_2O)_6]^{2+}$ and $(BF_6)^{2-}$ and packed in the way shown in Fig. 1. The greatest degree of order between two different orientational configurations for each of the complex ions occurs in the magnesium fluosilicate [4].

On the basis of structural the fluosilicates can be divided into two groups; the symmetry of high temperature phases for crystals with A = Ni, Zn, Co is determined as $R\bar{3}$ [7, 9] and respectively as $R\bar{3}m$, $P\bar{3}m1$, $P\bar{3}$ for those with A = Fe, Mn, Mg [4, 6, 10, 14, 15]. The fluosilicates except nickel and zinc undergo the improper ferroelastic phase transitions leading to the monoclinic $P2_1/c$ system [13]. The mechanism of transitions is described in terms of rotations of the metal-water and fluosilicate octahedra in neighbouring columns.

From the calorimetric data it has been found that the values of the entropy changes $\Delta S/R$ at the phase transitions are different for these two groups of crystals; a large value 0.7 or higher is characteristic for the first group and rather small value less than 0.5 for the second one [11, 12].

The structural model of high-temperature phase of $MgSiF_6 \cdot 6H_2O$ [4] involves an arrangement of two types of ordered domains (the space group $P\bar{3}$) built from the low temperature cell, that take the form of layers parallel to the hexagonal basal plane. Fig. 2 shows the arrangement of $(SiF_6)^{2-}$ anions surrounding the $[Mg(H_2O)_6]^{2+}$ cation in the monoclinic phase. For clarity the $[SiF_6]^{2-}$ octahedra above and below the cation have been omitted. This figure shows the two different orientations, labeled A and B, of the fluosilicate octahedra that are related to each other by a rotation about the hexagonal axis c_h or reflection in the mirror planes of the trigonal structure (marked by m).

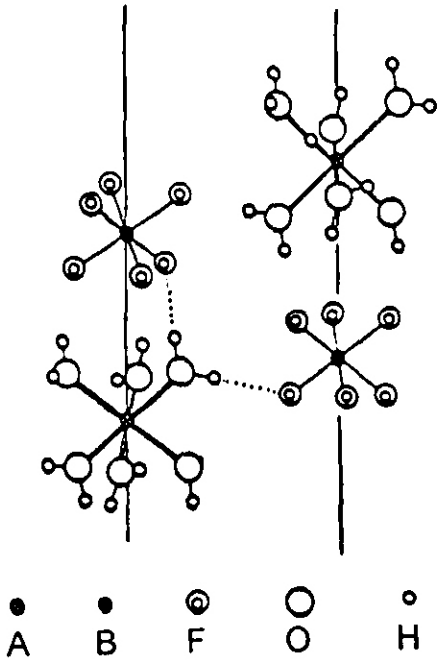

Fig. 1. Two neighbouring columns in the structure of $ABF_6 \cdot 6H_2O$ system [7]

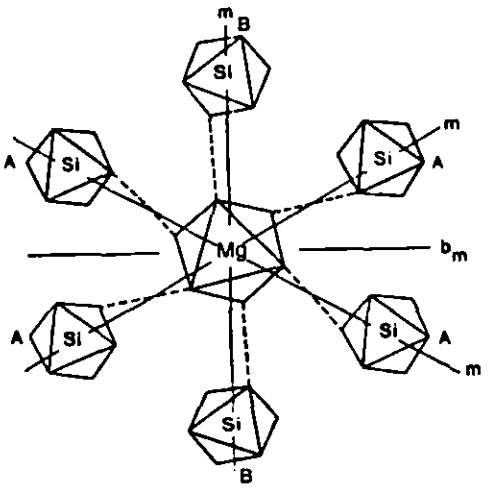

Fig. 2. The arrangement of anions (labeled Si) surrounding a cation (labeled Mg) in $MgSiF_6 \cdot 6H_2O$ as viewed down the pseudo-hexagonal axis c_h in the low temperature monoclinic phase (adapted from [13]). The B orientations are related to the A orientations by reflections in the mirror planes labeled m

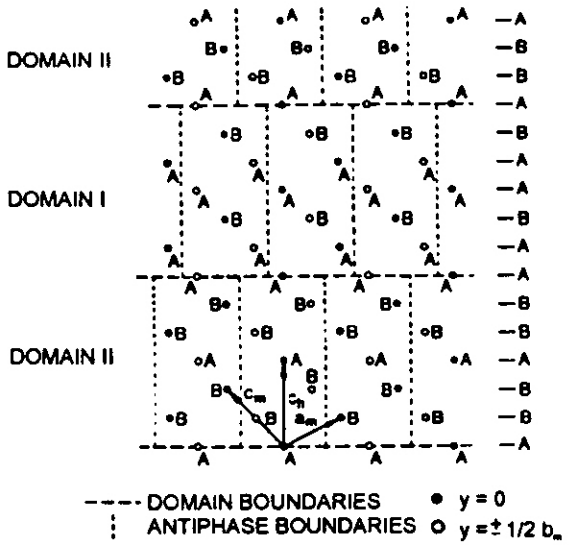

Fig. 3. Arrangement of the two orientational configurations A and B of one species of octahedral complex ion in the high temperature phase of MFS ($T > 300$ K). The projection is onto the hexagonal plane ($1.\bar{2}.0$) which contains the c_h axis as well as the monoclinic a_m and c_m axes. The elements of the low temperature monoclinic structure arranged periodically in antiphase within each domain are shown [4]

Figure 3 depicts the ordering of these inequivalent orientations, for one kind of the octahedral complex ion only ($[SiF_6]^{2-}$), in the high temperature phase. The other kind lies in the same columns along the hexagonal axis c_h, separated by $\pm\, c_h$ from their neighbours in the c_h direction (Fig. 1). One type of domain contains, for each kind of octahedral ion, two orientations A for each orientation B; the situation is reversed in the other type of domain. The overall stacking order along the c_h axis is AABAABABBABBAAB.... Thus, the whole structure consists of a coherent modulated arrangement of elements of the monoclinic structure that are commensurate with the lattice [4].

2. EPR LINESHAPE ANALYSIS

$MgSiF_6 \cdot 6H_2O$ undergoes the ferroelastic phase transition of first order to the monoclinic phase at $T_c = 298$ K [13]. The EPR studies of Mn^{2+} in this crystal [5] revealed that at temperatures above T_c the resonance lines are unusually broadened and their positions are limited by two edge singularities. Hence, for the first time, the conception about the existence of the intermediate incommensurate phase above T_c was postulated from the EPR studies.

The same ideas were presented by the other authors in the papers appearing later [16, 17]. Unfortunately, the simulated EPR spectra in the intermediate phase of the $MgSiF_6 \cdot 6H_2O$ crystal have been described incorrectly by two-linear and quadratic terms despite the fact that linear coefficients are not symmetry allowed for the magnetic field orientation chosen by them.

The new approach consistent with the symmetry requirements for the crystal orientation in the magnetic field describes satisfactorily the experimental EPR spectra in $MgSiF_6 \cdot 6H_2O$ in its high temperature phase [18]. The temperature evolution of the EPR spectra of Mn^{2+} admixture ions in $MgSiF_6 \cdot 6H_2O$ for a magnetic field parallel to the threefold axis of the crystal (pseudo-

hexagonal c_h) is shown in Fig. 4a. One can notice the broadening of the Mn^{2+} hyperfine structure lines followed by splitting of these lines while decreasing the temperature. The phase transition from a paraelastic to ferroelastic phase occurring at T_c = 299 K is observed in the EPR spectra through additional splitting of the resonance lines.

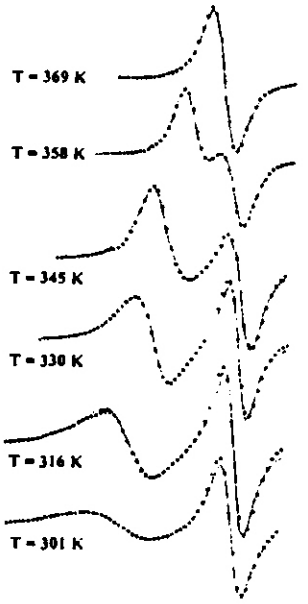

Fig. 4a. Temperature evolution of the EPR Mn^{2+} spectra lineshape (scattered points describe experimental spectra, solid line – theoretical simulated spectra)

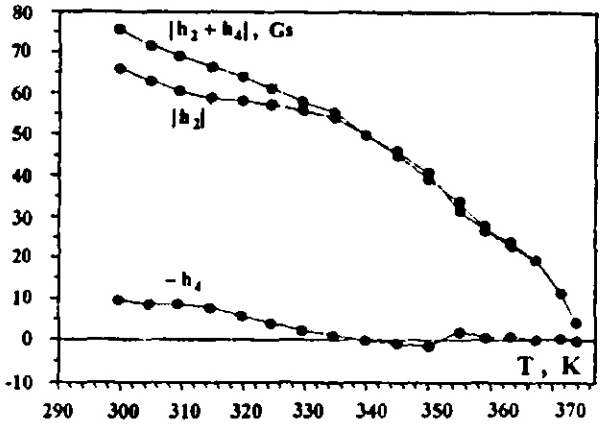

Fig. 4b. Temperature dependence of incommensurate modulation parameters h_2 and h_4 calculated from the experimental spectra

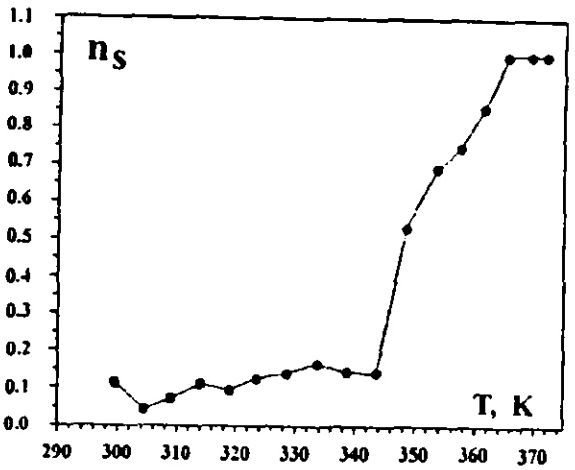

Fig. 4c. Temperature dependence of soliton density n_s for this model

The experimental Mn^{2+} EPR lineshape in the high temperature phase of MFSH has been interpreted in the terms of model involving an incommensurably modulated structure [18]. The resonance field of a given paramagnetic centre was expanded in powers of order parameter holding even terms up to fourth power. The temperature dependence of modulation parameters as well as the soliton density is shown in Fig. 4b and 4c, respectively. Basing on this model the simulated EPR spectra are presented in Fig. 4a.

Since neither rentgenographic nor neutronographic methods did reveal satellite reflections in the incommensurate positions the attempt to alternative approach to the interpretation of the EPR lineshape in this crystal in the framework of regular antiphase domain structure has been undertaken [19]. The considered model is based on assumption that the antiphase boundaries have a linear structure which is represented by the kink-solution:

$$Q(x) = Q_0 \tanh kx \tag{1}$$

where k^{-1} is the measure of domain wall thickness, the x-axis is normal to the APB plane and Q_0 is the value of the order parameter inside the two domains and the magnetic field can be expanded into the power series of the order parameter. For the quadratic case the resonance field distribution function $f(B)$ is given in the form [19]:

$$f(B) = \frac{2\pi\cosh^2 kx}{B_2 k \tanh \Phi(x)} = \frac{2\pi/k}{2B_2\sqrt{\dfrac{B - B_0}{B_2}\left(1 - \dfrac{(B - B_0)}{B_2}\right)}} \tag{2}$$

where B_2 is the is the quadratic term in this power series expansion.

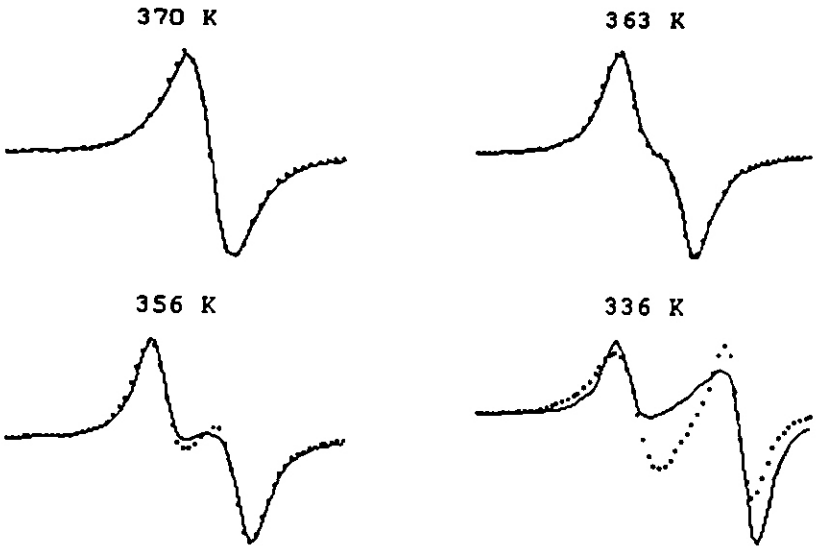

Fig. 5. The comparison between experimental (dotted line) and simulated (solid line) EPR lineshape in case of continuous domain wall model

The above resonance field distribution function allows to obtain the simulated EPR lines. Figure 5 presents the comparison between the simulated and experimental lines for Mn^{+2} centres in $Mg(SiF_6) \cdot 6H_2O$. Although the above model with a continuous variable allows to predict the splitting of the resonance lines and changes in the EPR lineshape it does not give a good agreement between the experimental and theoretical lines in a whole temperature range.

According to the structural model the domain width is comparable with the size of unit cell and the transient region (domain wall) is a result of the error in the stacking only of the single plane e. g. the first plane A in the domain I in Fig. 3. So the discrete domain wall model rather than continuous one should be used to describe the observed EPR spectra in MFSH.

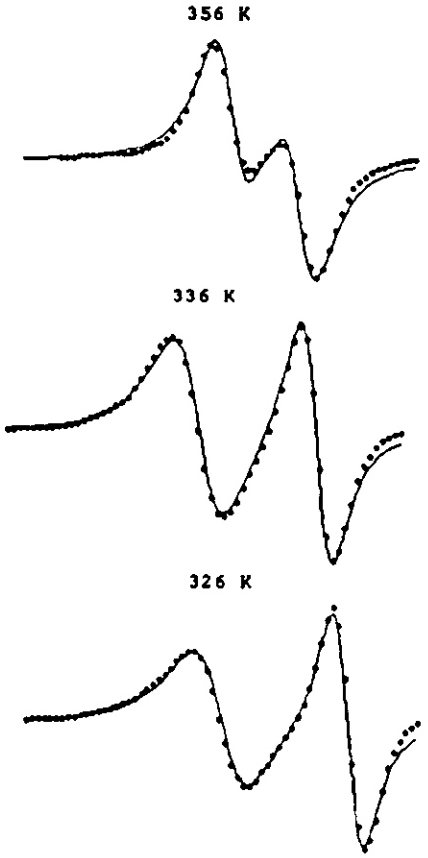

Fig. 6. The comparison between experimental (dotted line) and simulated (solid line) EPR lineshape in case of narrow domain wall model. The fitting parameters of two (Lorentzian) constituent lines are: B_1, B_2 – resonance fields; $\Delta B(1)$, $\Delta B(2)$ – the linewidths; A_2/A_1 – the amplitude ratio:
356 K: 186.8 mT, 184.7 mT; 0.6 mT, 0.6 mT; $A_2/A_1 = 1$
336 K: 187.6 mT, 183.9 mT; 0.5 mT, 0.8 mT; $A_2/A_1 = 1.82$
326 K: 187.8 mT, 183.6 mT; 0.5 mT, 0.9 mT; $A_2/A_1 = 1.86$

In the high temperature phase one could recognize two kinds of the $[Mg \cdot 6H_2O]$ centres – one possessing the inversion centre localised inside the antiphase domains and the another without this symmetry element [4, 20]. The latter is situated near the domain boundary and has the coordination neighborhood belonging to the two adjacent domains, so it could be assumed that this centre is situated in the thin domain wall of thickness equal to the distance between two nearest planes (e. g. AA in Fig. 3).

The manganese ions could be built into these two sites (with and without the inversion centre) thus giving two different paramagnetic complexes what can be seen in the EPR spectra as two

different resonance lines. In this model changes in the domain thickness should lead to changes in the relative intensity of these resonance lines. Moreover, the centres assumed to originate from the domain walls could give broader EPR lines as the result of compensation of strains due to the fault in the planes stacking.

Taking into consideration this model the simulated EPR spectrum was approximated by two lines: one narrow and another much broader as shown in Fig. 6. The above model stops working in the vicinity of temperature 350 K. The crystal starts loosing the crystalline water around this temperature [21] what would lead to significant changes of the EPR spectrum.

It seems that the approach presented is consistent with the structural model of $MgSiF_6 \cdot 6H_2O$ above T_c derived from the X-ray and neutronographic studies [4, 15].

References

[1] K. Fujiwara, J. Phys. Soc. Jap. 12, 7 (1957).
[2] G. Jehanno and P. Perio, J. Phys. France 23, 854 (1962).
[3] P. Bak, Rep. Prog. Phys. 45, 587 (1982).
[4] G. Chevrier and G. Jehanno, Acta Crystallogr. A35, 912 (1979).
[5] A. M. Ziatdinov, V. G. Kuryavyi, R. L. Davidovich, Sov. Phys. Solid State 27, 1288 (1985); A. M. Ziatdinov, V. G. Kuryavyi, Ferroelectrics 143, 99 (1993).
[6] W. C. Hamilton, Acta Cryst. 15, 353 (1962).
[7] M. Bose, K. Roy, A. Ghoshray, Phys. Rev. B35, 6619 (1987).
[8] B. Ghosh, N. Chattarjee, A. N. Das, A. Chatterjee, J. Phys. C12, 3283 (1979).
[9] S. Ray, A. Zalkin, D. H. Templeton, Acta Crystallogr. B29, 2741 (1973); S. Ray, G. Mostafa, Zeit. Kristallogr. 211, 368 (1996).
[10] E. Kodera, A. Torii, K. Osaki, T. Watanabe, J. Phys. Soc. Jap. 32, 863 (1972).
[11] R. D. Weir, K. E. Halstead, L. A. K. Staveley, Discuss. Faraday Soc. 69, 202 (1980); J. Chem. Soc. Faraday Trans. II 81, 189 (1985).
[12] I. N. Flerov, M. V.Gorev, K. S. Aleksandrov, M. L. Afanasjev, J. Phys: Condens. Matter 4, 91 (1992).
[13] S. Syoyama and K. Osaki, Acta Cryst. B28, 2626 (1972).
[14] G. Jehanno and F. Varret, Acta Crystallogr. A31, 857 (1975).
[15] G. Chevrier and G. Jehanno, Acta Cryst. A37, 578 (1981).
[16] R. Hrabański, Ferroelectrics 124, 333 (1991).
[17] M. Suhara, T. Bandoh, T. Kitai, Phase Transitions 32, 111 (1992).
[18] P. G. Skrylnik and A. M. Ziatdinov, Bull. Mag. Res. 19-20, 83 (1999).
[19] W. Zapart and M. B. Zapart, Bull. Mag. Res. 19, 34 (1999).
[20] D. C. Price, Can. J. Phys. 65, 1280 (1987).
[21] I. N. Flerov, M. V. Gorev, S. V. Melnikova, M. L. Afanasjev, K. S. Aleksandrov, Fiz. Tverd. Tela 33, 1921 (1991).